Advancing Data Assimilation and Uncertainty Quantification for CO2 Sequestration through AI-Hybrid Methods

Seabra, G. Serrao; Mücke, N. T.; Silva, V. Luiz Santos; Voskov, D.; Vossepoel, F.

DOI
10.3997/2214-4609.202437083

Publication date
2024

Document Version
Final published version

Published in
European Conference on the Mathematics of Geological Reservoirs, ECMOR 2024

Citation (APA)
Seabra, G. S., Mücke, N. T., Silva, V. L. S., Voskov, D., & Vossepoel, F. (2024). Advancing Data Assimilation and Uncertainty Quantification for CO2 Sequestration through AI-Hybrid Methods. In *European Conference on the Mathematics of Geological Reservoirs, ECMOR 2024* (Vol. 2, pp. 886-908). EAGE. https://doi.org/10.3997/2214-4609.202437083

Advancing Data Assimilation and Uncertainty Quantification for CO2 Sequestration through AI-Hybrid Methods

G. Serrao Seabra[1,2], N. T. Mücke[3,4], V. Luiz Santos Silva[2,5], D. Voskov[1,6], F. Vossepoel[1]

[1] TU Delft; [2] Petroleo Brasileiro S.A.; [3] Centrum Wiskunde & Informatica; [4] Mathematical Institute Utrecht University; [5] Imperial College London; [6] Stanford University

Summary

In this comprehensive study, we discuss a novel approach to enhance data assimilation and uncertainty quantification in the field of Geological Carbon Sequestration (GCS). We specifically address the complexities of channelized reservoirs, which pose significant challenges due to non-Gaussian permeability distributions and the intricate non-linear physics of CO2 injection processes. Our innovative method integrates Fourier Neural Operators (FNOs) and Transformer UNet (T-UNet) with advanced data assimilation techniques - the Surrogate-based Hybrid Ensemble Smoother with Multiple Data Assimilation (SH-ESMDA) and the Surrogate-based Hybrid Randomized Maximum Likelihood (SH-RML). These techniques make use of the very efficient computation of gradients that neural networks provide and they not only improves the speed of data processing but also enhances the accuracy of predictions in synthetic data assimilation experiments for GCS applications. A key element of our approach is the use of proxy models alongside high-fidelity simulations, ensuring the consistency and reliability of physical posterior distributions. We utilized Alluvsim for detailed geological modeling and the Delft Advanced Research Terra Simulator (DARTS) for comprehensive fluid flow simulations, providing a comprehensive understanding of reservoir dynamics. A synthetic case study on a channelized reservoir model for CO2 sequestration demonstrates the effectiveness of these methods, with improvements in predicting CO2 plume migration and pressure dynamics within the reservoir. The results of our study show that the integration of FNOs and T-UNet with SH-ESMDA and SH-RML leads to enhanced prediction capabilities, particularly in the challenging context of channelized reservoirs. The SH-ESMDA method proves to be highly efficient in speeding up the data assimilation process without compromising accuracy, while SH-RML demonstrates a more effective history matching compared to standard Ensemble Smoother with Multiple Data Assimilation (ESMDA) techniques, indicating a robust strategy for assimilating complex data. This research not only contributes to the realm of GCS but also presents a novel solution for the integration of artificial intelligence with traditional methodologies that can be applied in various fields where data assimilation and uncertainty quantification are crucial. Our study paves the way for future advancements in this domain, highlighting the potential of AI-driven techniques in enhancing data assimilation and uncertainty quantification for GCS projects.

Introduction

The global urgency to mitigate climate change has propelled Carbon Capture, Utilization, and Storage (CCUS) strategies, particularly Geological Carbon Storage (GCS), to the forefront of emissions reduction efforts (Ringrose and Meckel, 2019; IEA, 2022). As these initiatives expand, they face dual challenges: maximizing storage efficiency and minimizing associated risks. This study explores innovative approaches to address these challenges through the integration of advanced data assimilation (DA) techniques and machine learning (ML) in GCS projects. The complexity of GCS operations is exemplified by projects like the water alternating gas (WAG) injection in Brazil's Pre-Salt region. Despite sequestering 20 Mton of CO_2 across four major carbonate formations over a decade, this project illustrates the gap between current capabilities and the ambitious targets set by organizations like the International Energy Agency (Nunes et al., 2022). The geological complexities of storage sites, often characterized by fractured carbonate rocks and channelized reservoirs, present significant obstacles to efficient and safe CO_2 storage (Burchette, 2012; March et al., 2018).

A critical aspect of GCS management is pressure control during CO_2 injection. Improper pressure management can lead to severe consequences, including induced seismicity and caprock failure, potentially compromising the entire storage system (Li and Liu, 2016; Zoback and Gorelick, 2012; Rutqvist, 2012; White and Foxall, 2016). Recent research has proposed innovative solutions, such as the use of horizontal wells, to enhance injection control and storage security (Machado et al., 2023). The success of GCS projects depends on the synergy between detailed geological modeling, sophisticated reservoir simulation, and advanced data assimilation techniques. Tools like Alluvsim enable the creation of complex geological models that capture key features of natural deposition processes (Pyrcz et al., 2009). High-fidelity reservoir simulators, including CMG GEM (CMG, 2023), SLB Eclipse (Schlumberger, 2023), DuMux (DuMux, 2023), GEOSX (GEOSX, 2023), and DARTS, are employed to simulate CO_2 injection dynamics. DARTS, for instance, utilizes operator-based linearization (OBL) for efficient simulations, though integrating these simulators into DA frameworks remains computationally challenging (Lyu and Voskov, 2023; Khait and Voskov, 2017).

Forecasting reservoir behavior under uncertainty, while constrained by data and considering physics-based models and prior knowledge, can be achieved using DA methods. These methods can be categorized into different types: some are based on ensemble methods such as Ensemble Kalman Filters and Smoothers, variational methods like Randomized Maximum Likelihood and 4D-Var, and fully nonlinear methods comprising Particle Filters and Markov Chain Monte Carlo (Evensen et al., 2022; Tarantola, 2005). Ensemble methods offer computational efficiency and flexibility, while variational methods achieve better convergence. However, variational methods require gradient computations Tian et al. (2024a,b), and fully nonlinear methods provide high accuracy but demand significant computational resources. Recent advancements have integrated machine learning (ML) with DA in an attempt to overcome some of these difficulties (Buizza et al., 2022; Silva et al., 2023). Bridging these traditional DA methods with modern computational techniques, recent innovations have introduced machine learning (ML) into the data assimilation framework to enhance its effectiveness (Buizza et al., 2022; Silva et al., 2023). This integration leads to "Data Learning" approaches that leverage ML's prowess in pattern recognition to complement DA's strengths in fusing these patterns with dynamic physical models and constraints. Such hybrid approaches, which synergistically combine DA and ML, are proving particularly useful in challenging applications like CO_2 injection, where understanding complex reservoir dynamics is crucial (Buizza et al., 2022; Cheng et al., 2023; Brajard et al., 2021; Tarrahi et al., 2015; Tadjer and Bratvold, 2021). This convergence of traditional and modern computational techniques marks a significant advance in the field of reservoir management and uncertainty quantification.

In the context of using machine learning as surrogate models for data assimilation in reservoir simulations, UNets have demonstrated strong performance when used as surrogate models for data assimilation in reservoir simulations, making them a popular choice among researchers (Wen et al., 2021a; Zhang et al., 2021; Pintea et al., 2021; Ronneberger et al., 2015; Taccari et al., 2022). This approach has further advanced with the incorporation of transformers into UNets, enhancing their segmentation capabilities (Li et al., 2023; AlSalmi and Elsheikh, 2023). Additionally, Fourier Neural Operators (FNOs) are increasingly applied to model complex interactions in CO_2 injection scenarios, offering significant advancements over traditional surrogate modeling techniques. These operators handle the complexities associated with the high-dimensional spaces of this problem, often required for CO_2 sequestration simulations. Unlike traditional models that necessitate extensive training datasets, FNOs excel in environments where data may be sparse or expensive to obtain. Their spectral approach allows them to capture long-range dependencies and intricate patterns in data, which is important for accurately predicting the behavior of the reservoir (Li et al., 2020; Wen et al., 2022; Witte et al., 2023). There are also recent developments of surrogate models intended to replace conventional physics-based methods in DA, though these require extensive training data and struggle with fully capturing subsurface complexities Tang et al. (2022); Wen et al. (2021b); Sun and Durlofsky (2019); Agogo et al. (2022); Dong et al. (2021). To mitigate these challenges, hybrid models that merge ML and physics-based approaches have been framed to achieve a balance between accuracy and computational efficiency, enhancing predictability under variable conditions despite facing integration limitations due to differing model parameterizations (Tang and Durlofsky, 2022; Korondi et al., 2020; de Brito and Durlofsky, 2020).

In our approach, we begin with the conventional Ensemble Smoother with Multiple Data Assimilation (ESMDA) using DARTS to conduct precise simulations of channelized reservoirs designed with Alluvsim. The complexity and non-Gaussian parameter distribution in these simulations presents significant challenges for data assimilation. To improve the conventional ESMDA, we assess two machine learning surrogate models: the first based on FNOs, and the second utilizing a Transformer-based UNet (T-UNet). Our comparative analysis indicates that FNOs have a marginal superiority over T-UNets, especially with smaller data sets. Building on this, we evaluate two hybrid approaches that merge data assimilation with these ML surrogates, recently proposed by Seabra et al. (2024). The first approach, which we call Surrogate-based hybrid ESMDA (SH-ESMDA), integrates the ML surrogates to accelerate the ESMDA process by over 50 %. The second approach, the Surrogate-based Hybrid Randomized Maximum Likelihood (SH-RML), utilizes ML surrogates for gradient calculations within a variational framework and employs DARTS to generate the posterior curves. SH-RML demonstrates superior history-matching capabilities compared to both ESMDA and SH-ESMDA. Our key contributions include:

- The evaluation of two distinct ML surrogate models, specifically FNO and T-UNet, within a channelized reservoir environment for CO_2 storage.
- The assessment of two innovative hybrid methodologies, SH-ESMDA and SH-RML, which integrate ML with ensemble and variational data assimilation techniques, respectively, proposed by Seabra et al. (2024). The former significantly speeds up the data assimilation process, while the latter facilitates variational data assimilation.
- Ensuring that the high-fidelity physics solutions are maintained in all posterior analyses.
- Demonstrating the adaptability of these methods to a range of physical systems beyond CO_2 sequestration.

Overview of the Reservoir Model for CO_2 Injection

Our research utilizes Alluvsim to generate a diverse ensemble of channelized reservoir models, incorporating a wide range of geological parameters to represent the complex features of these formations. The modeling process involves the systematic variation of multiple elements to create a spectrum of possible reservoir characteristics. We include avulsion probability as a parameter to represent the potential for channel migration, while varying aggradation levels simulates different scenarios of vertical sediment accumulation. Channel orientations are diversified to reflect the range of patterns observed in natural systems. The models also incorporate variations in channel thickness, width-to-thickness ratios, and levee dimensions to represent different sedimentary structure morphologies. Channel sinuosity is varied to depict different degrees of meandering in fluvial systems. To account for the heterogeneity of reservoir rock properties, we introduce variations in facies characteristics across the models. This comprehensive approach results in a broad ensemble of geological realizations that capture the inherent variability and complexity of natural reservoir systems. The diversity of these simulated reservoirs is illustrated in Figure 1, which displays a selection of the generated permeability distributions.

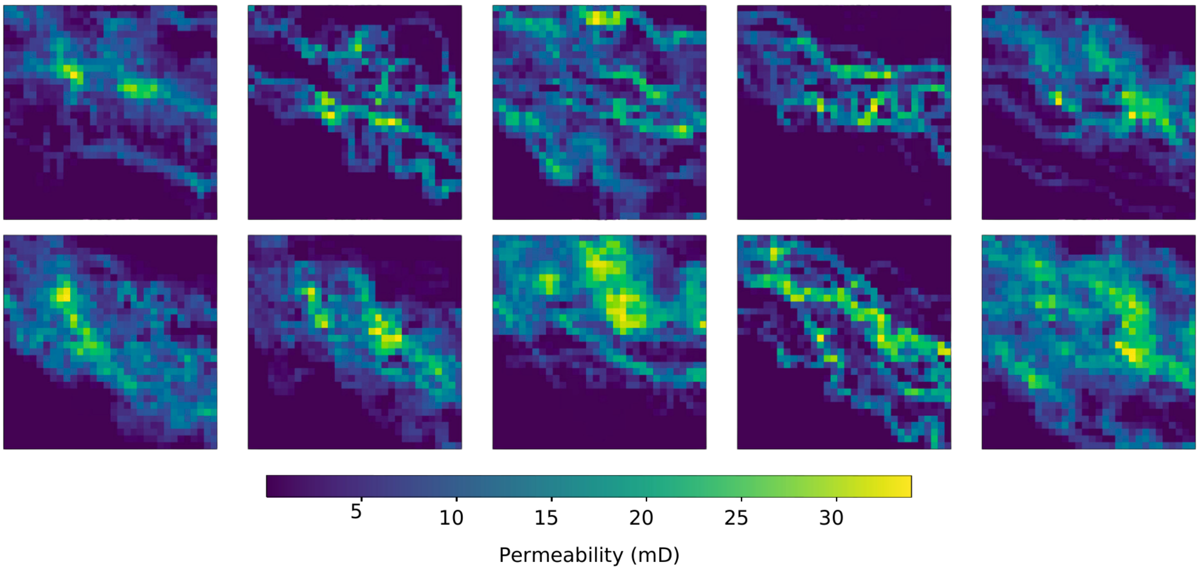

Figure 1 *Permeability maps of ten models from the dataset.*

These models are used to simulate CO_2 injection with DARTS, which has been applied by several researchers for complex flow dynamics through porous media (Khait and Voskov, 2017; Pour et al., 2023; Chen and Voskov, 2020; Wapperom et al., 2023; Lyu and Voskov, 2023; DARTS, 2024). The simulation parameters, such as gas phase viscosity and mixture densities, are calculated using models from the literature, and a hybrid EOS model is utilized for dissolution processes (Fenghour et al., 1998; Wapperom et al., 2023). The simulation setup, illustrated in Figure 2, comprises a centrally located well within a computational grid that mimics the geological model. This configuration is designed for CO_2 injection and subsequent monitoring of its spatial distribution. The figure specifically displays the final pressure and CO_2 molar fraction for a single sample simulation, providing crucial insights into the system's behavior under the defined conditions. These simulations, despite neglecting certain phenomena like capillary pressure effects for simplification, effectively capture the multiphase flow dynamics critical to understanding CO_2 migration and trapping in the studied reservoir (Wapperom et al., 2023).

The simulations highlight the complex behavior of pressure and CO_2 fronts within the reservoir, illustrating how pressure changes precede the CO_2 front, suggesting the potential of pressure monitoring as an early detection system for subsurface changes. Besides the significant risks associated with pressure monitoring, there is also the advantage of early warning capabilities for subsurface changes.

Neural Networks as Surrogate Forward Models

Our approach involves constructing surrogate models using neural networks, which are trained in an offline stage and deployed in an online stage to simulate fluid behavior. These models, particularly effective due to their ability to approximate complex nonlinear functions, are ideal for nonlinear and hyperbolic problems where traditional linear dimensionality reduction methods tend to fall short (Quarteroni et al., 2015; Hesthaven et al., 2016; Ohlberger and Rave, 2015; Mücke et al., 2021; Li et al., 2020; Geneva and Zabaras, 2022). For the offline stage, we generate high-fidelity solutions as training data. The neural networks, specifically T-UNet and FNOs, are then trained on these data. The forward model in our simulations maps input parameters such as permeability and porosity, represented by K and ϕ, and injection rate q, to outputs like pressure and CO_2 molar fraction. The parameter space and state trajectories are formally defined as $z = (K, \phi, q)$ in Z and $d = (p, f)$ in V, respectively. The mapping is accomplished by the surrogate forward model $\hat{G}$, which approximates the true forward map G, described

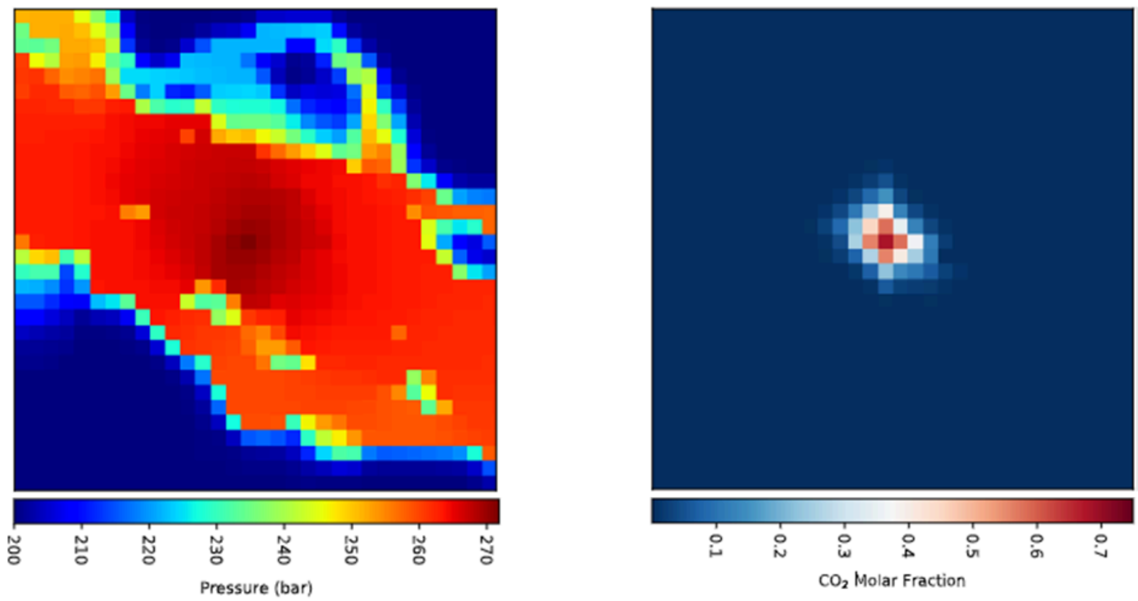

Figure 2 *Simulation results using DARTS. Left panel: Pressure distribution (Bar); Right panel: CO_2 molar fraction.*

by:

$$G : Z \to V, \quad z \mapsto d, \quad \text{and} \quad \hat{G} : Z \to V, \quad z \mapsto d, \quad \hat{G}(z) \approx G(z). \tag{1}$$

This approximation avoids solving PDEs directly by employing a neural network parametrized by weights θ, trained to minimize a loss function reflecting the difference between the predicted and actual outputs, using methods like stochastic gradient descent optimized by algorithms such as the Adam optimizer (Kingma and Ba, 2014).

In summary, the surrogate model training involves creating and using a training set S_{train} from the high-fidelity model outputs, focusing on optimizing the neural network to accurately mimic the reservoir's fluid dynamic behaviors under varied conditions. Transitioning from this setup, our study explores the application of advanced neural network architectures. We investigate the UNet structure, a design initially conceived for medical image analysis, which we have now adapted and applied to GCS scenarios. This novel application represents one of the first instances of UNet's utilization in the field of carbon storage modeling. This architecture compresses the input dimension to a bottleneck through a series of convolutional layers and then expands it back to the original dimension using upscaling layers, enriched by concatenating feature information from earlier layers (Ronneberger et al., 2015; AlSalmi and Elsheikh, 2023). In the context of GCS, we leverage the UNet framework to integrate crucial spatial parameters such as porosity and permeability with temporal data like injection rates directly within the bottleneck layers, thereby enhancing the model's efficiency in capturing complex subsurface behaviors, as depicted in Figure 3 (Seabra et al., 2024).

On the other hand, FNOs introduced by Li et al. (2020) handle parametric PDE problems by learning functional mappings rather than traditional Euclidean mappings, rendering them resolution-invariant. FNOs transform inputs via the Fourier transform, perform operations in the Fourier space, and then transform them back, which efficiently captures the data's inherent periodicities. The structure of an FNO layer is described as:

$$a^{n+1}(x) = \sigma\left(Wa^n(x) + \mathscr{F}^{-1}(R \cdot (\mathscr{F} a^n))(x)\right), \tag{2}$$

where σ denotes an activation function, and W and R represent trainable weights, with Fourier operations truncated to a limited number of modes for efficiency. The architecture of the FNO is visualized in Figure 4.

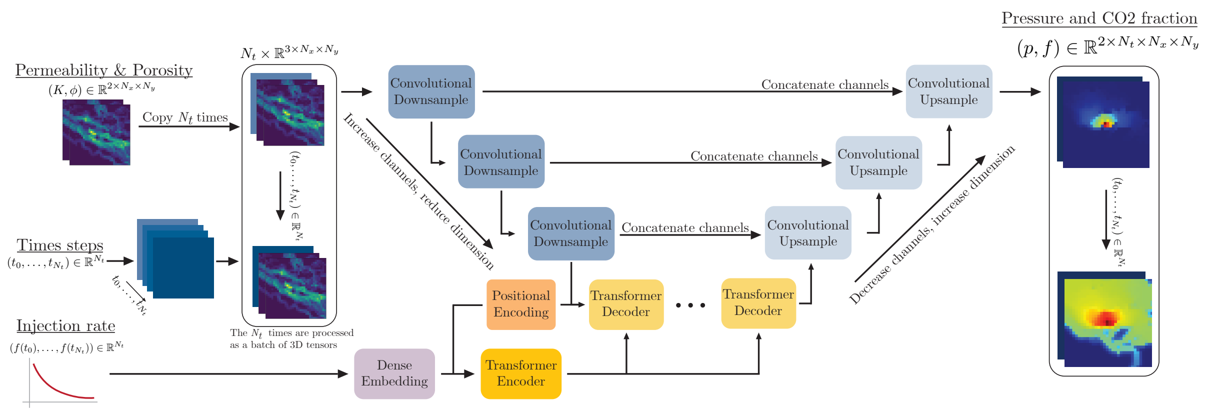

Figure 3 *T-UNet setup applied, which combines convolutional layers with transformer modules to optimize the handling of spatial and temporal data (Seabra et al., 2024)*

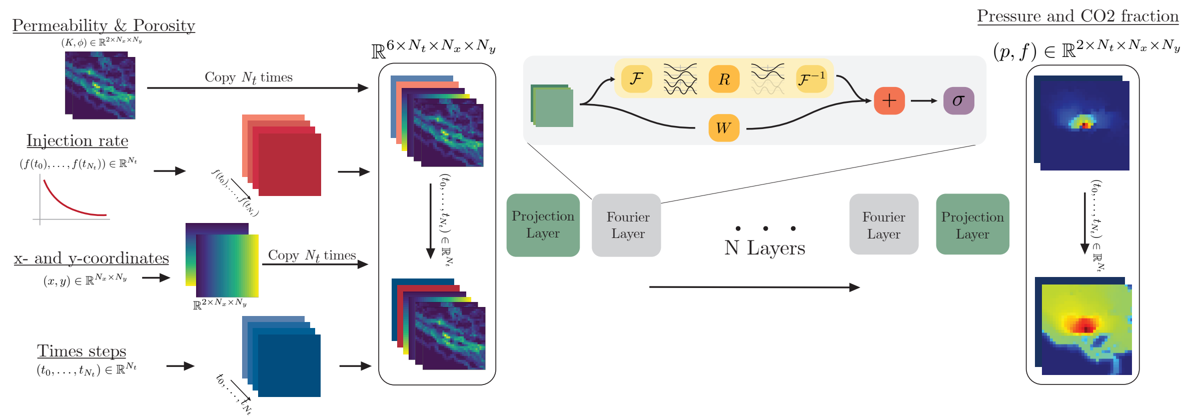

Figure 4 *Fourier Neural Operator setup used in our study, which leverages Fourier transformations to efficiently process parametric PDEs. (Seabra et al., 2024)*

Both architectures, T-UNet and FNO, are utilized to approximate the high-fidelity forward model, G. The T-UNet benefits from its ability to integrate temporal information with spatial data effectively, while FNOs offer a direct approach to function space modeling, ideal for handling complex parametric PDEs. However, FNOs require more memory due to their handling of data as 3D tensors, reflecting both spatial and temporal dimensions. Both models have been trained to optimize performance using a loss function that combines the L^2-norm for accuracy and a regularization term to prevent overfitting:

$$L(\hat{G}, S_{\text{train}}) = \frac{1}{N_s} \sum_{i=1}^{N_s} ||\hat{G}(z_i) - d_i||_{L^2}^2 + \lambda ||\theta||_2^2, \tag{3}$$

where L^2 represents the norm over a function space, a suitable metric for the continuous nature of the functions we are modeling.

Both FNO and T-UNet were trained using the DARTS simulator outputs to predict subsurface pressure and CO_2 molar fraction. For the FNO model, a sensitivity analysis was performed on the Width and Modes parameters, whereas for the T-UNet model, a fixed set of parameters was used. The models were evaluated based on RMSE, particularly for training sizes ranging from 100 to 1000 samples. Results indicate a slight edge for FNO in scenarios with smaller datasets, which is crucial for efficient data assimilation. The RMSE metrics for pressure are shown in Figure 5, and the RMSE metrics for CO_2 molar fraction are shown in Figure 6.

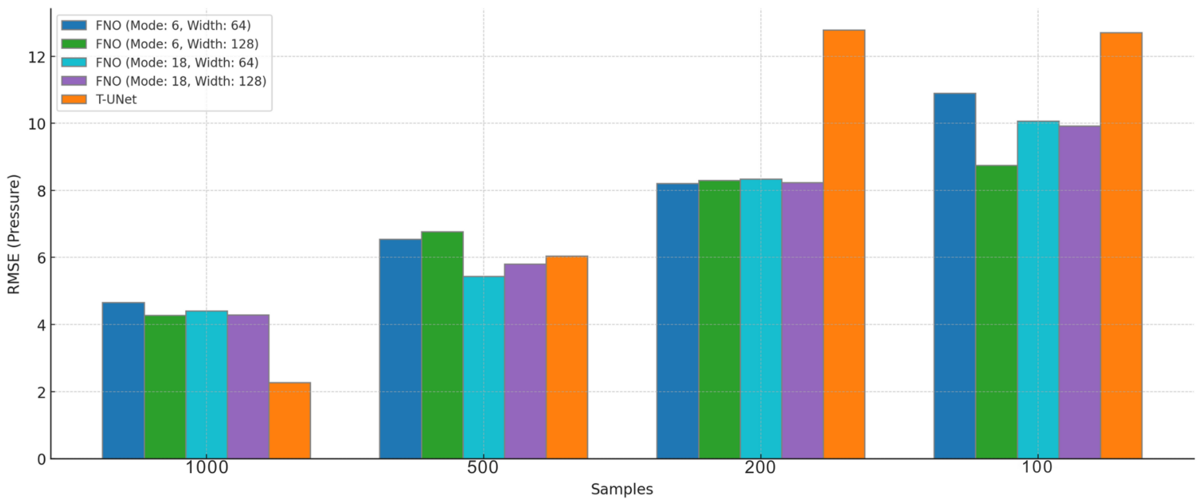

***Figure 5** Test RMSE Metrics for pressure (bars)*

In Figure 7, we compare the final pressure distributions for two different samples, utilizing DARTS, FNO, and T-UNet models. The top row of the figure illustrates the pressure distribution for the first sample, while the bottom row presents the second sample. For each sample, the left column shows the results from DARTS, the middle column displays the FNO predictions, and the right column contains the T-UNet predictions. Both neural networks exhibit strong agreement with the DARTS outputs, highlighting their capability to capture the complex subsurface pressure dynamics. This comparison underscores that both FNO and T-UNet can effectively match the high-fidelity simulator results, validating their application for reservoir modeling.

Figure 8 presents the pressure evolution over time for two different samples, labeled as (A) low pressure sample and (B) high pressure sample. Each plot compares the results from three different models: DARTS, FNO, and T-UNet, with pressure values recorded at the coordinates (x=16, y=16) for each time step. In both samples, the DARTS and FNO models show a smooth and continuous increase in pressure, indicating consistent predictions. The T-UNet model, however, exhibits a less smooth pressure evolution, particularly evident in the low pressure sample (A). This difference in smoothness is expected due to the inherent design of the models. The FNO model is designed to handle function space modeling with a smoother temporal response, which aligns with the observed results. On the other hand, the T-UNet

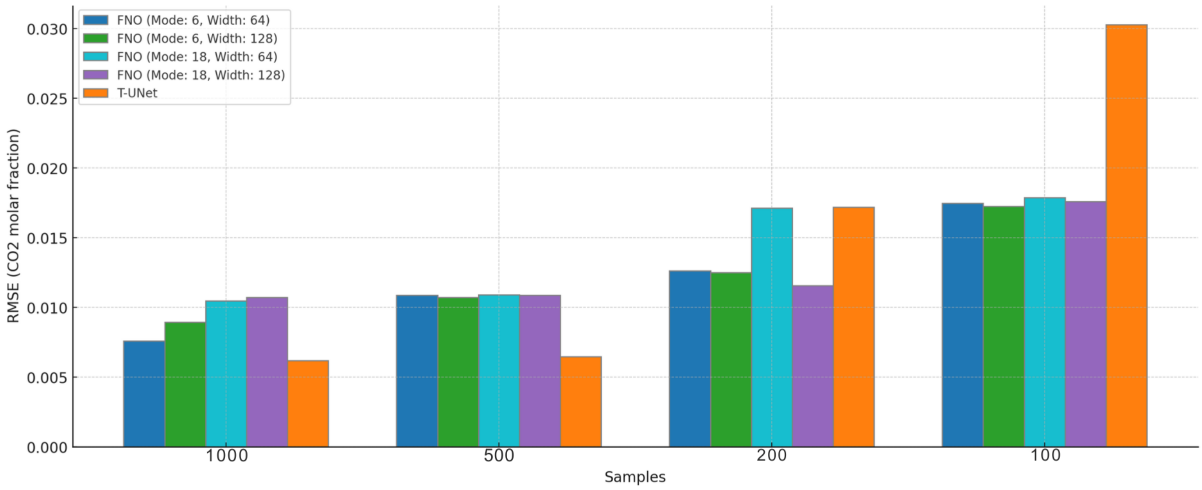

Figure 6 *Test RMSE Metrics for CO_2 molar fraction*

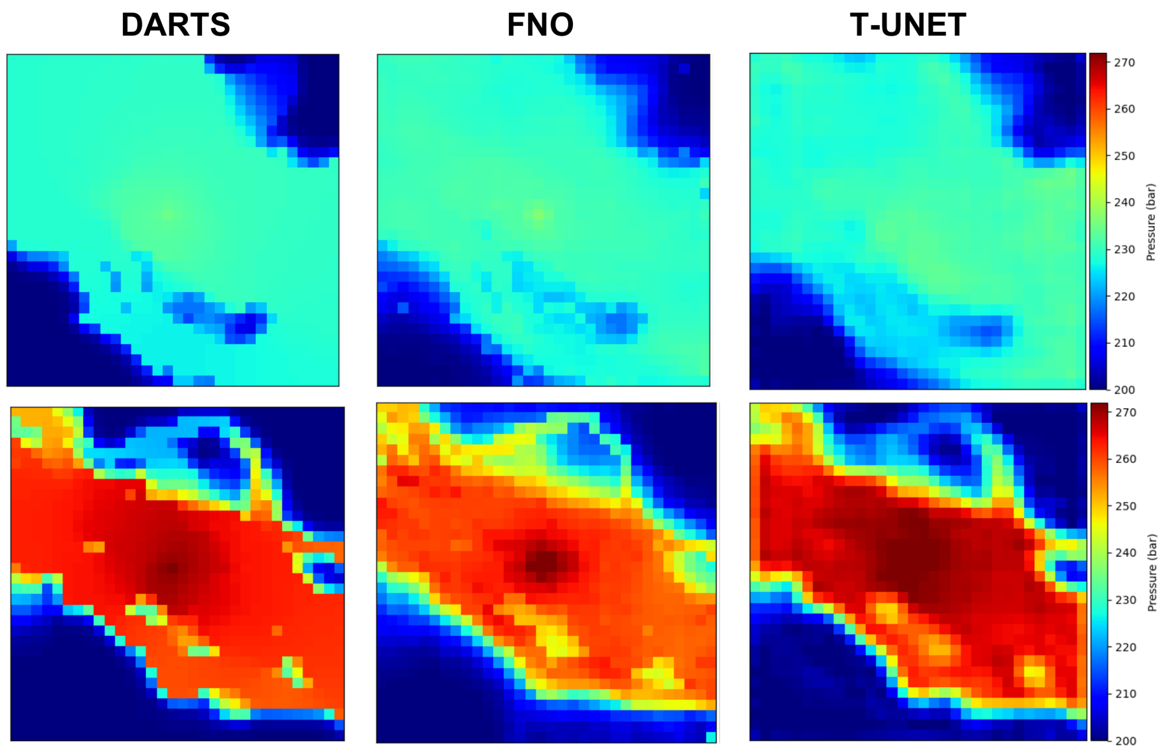

Figure 7 *Pressure distributions for a test case using DARTS, FNO, and T-UNet predictions.*

model, while effective in integrating temporal and spatial data, may produce slightly less smooth results due to its architecture and training process. Despite these differences, all models demonstrate a similar overall trend in pressure evolution, validating their effectiveness in subsurface pressure prediction.

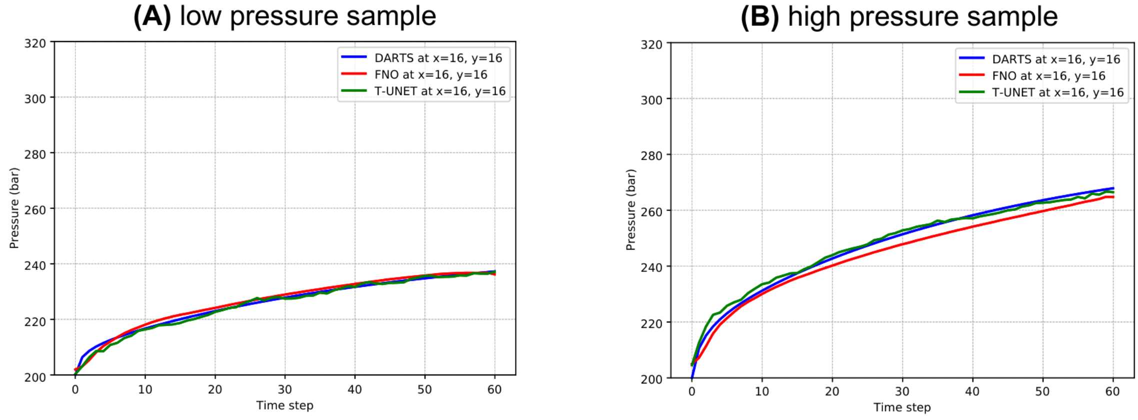

Figure 8 *Pressure evolution over time for two different samples using DARTS, FNO, and T-UNet models. (A) Low pressure sample. (B) High pressure sample.*

Data Assimilation with ESMDA and RML

Data assimilation (DA) techniques enhance the accuracy of reservoir simulations by integrating observational data with computational models. The methods evaluated in this study build upon two conventional DA methods, ESMDA and RML, each offering benefits and challenges.

ESMDA is an ensemble-based DA approach designed to iteratively perform ensemble updates through multiple data assimilation steps. This method is largely applied, however has some limitations, particularly when dealing with complex environments like GCS where non-linearities and non-Gaussian error distributions often complicate the data assimilation process. In ESMDA, the sensisity of the states in regards to the variations of the parameters are approximated by the ensemble response. ESMDA adjusts the ensemble by applying multiple Gauss-Newton corrections to better match the available data, described by Emerick and Reynolds (2013a). The update formula for each ensemble member z_j^a is:

$$z_j^a = z_j^f + C_{ZD}^f \left(C_{DD}^f + \alpha_i C_D \right)^{-1} \left(d_j - G(z_j)^f \right), \tag{4}$$

where z_j^f denotes the forecast parameters of the j^{th} ensemble member, C_{ZD}^f and C_{DD}^f are the forecast cross- and auto-covariance matrices, α is a scaling factor, and d_j and $G(z_j)^f$ represent the perturbed and forecasted observations, respectively (Emerick and Reynolds, 2013b).

RML, a variational DA method, aims to approximate the posterior distribution by minimizing a cost function that quantifies discrepancies between model predictions and observed data. It uses gradient-based optimization to adjust model parameters, providing a potential for higher accuracy and better convergence within specified solution spaces when compared to ESMDA, as long as the gradients are computed accurately. The cost function for RML is expressed as:

$$J(z_j) = (z_j - z_j^{\text{prior}})^T C_{ZZ}^{-1} (z_j - z_j^{\text{prior}}) + (G(z_j) - d_j)^T C_{DD}^{-1} (G(z_j) - d_j), \tag{5}$$

where z_j^{prior} and d_j represent the prior model parameters and perturbed observed data for the j^{th} ensemble member, respectively (Oliver et al., 1996).

Both ESMDA and RML are applied to adjust reservoir parameters such as permeability and porosity based on pressure data from monitoring locations. Implementing these advanced DA techniques ensures that our simulation outputs align closely with real-world observations, facilitating a thorough and accurate history matching process essential for reliable GCS studies.

Hybrid Data Assimilation Techniques

Hybrid data assimilation techniques aim to merge the computational advantages of machine learning (ML) surrogates with the accuracy of traditional ensemble and variational data assimilation methods. These methods are particularly effective in GCS simulations where computational efficiency and accuracy are paramount.

Surrogate-based Hybrid ESMDA (SH-ESMDA)

SH-ESMDA is a novel approach that incorporates ML surrogates within the "Data Learning" framework, as highlighted by Buizza et al. (2022). This method leverages ML models to approximate the forward model during the intermediate steps of the ESMDA process. The key motivation behind SH-ESMDA is to balance the trade-offs between computational efficiency and the robustness of traditional DA methods. The detailed steps of SH-ESMDA include:

- **Prior Dataset Generation**: Create a dataset of channelized permeability models using Alluvsim and simulate CO_2 injection using the DARTS simulator.
- **Surrogate Model Training**: Train a surrogate ML model, such as FNO or T-UNet, on the generated dataset. This model acts as a computationally efficient proxy to the high-fidelity DARTS simulations during the intermediate assimilation steps.
- **ESMDA Integration**: Utilize the trained surrogate model within the ESMDA framework to perform multiple assimilation cycles efficiently. The surrogate is used to estimate the forward model outputs, which are necessary for updating the ensemble predictions at each assimilation step.
- **Posterior Computation**: After employing the surrogate in the intermediate steps, the final assimilation step reverts to using the high-fidelity DARTS simulations to ensure the accuracy of the final model parameters.

This method significantly accelerates the ESMDA process by reducing the dependency on computationally intensive high-fidelity model simulations, thus allowing more frequent updates and iterations within practical time constraints.

Surrogate-based Hybrid RML (SH-RML)

Building on the concept of integrating ML surrogates, SH-RML adapts these models within the RML framework to enhance variational data assimilation. This approach is particularly beneficial in scenarios where traditional RML would require extensive computational resources:

- **Surrogate Model Utilization**: Similar to SH-ESMDA, SH-RML employs pre-trained ML surrogates to approximate the behavior of the forward model, thereby facilitating the initial optimization of the RML cost functions.
- **Gradient Computation and Optimization**: By leveraging the surrogate model's ability to provide gradients through automatic differentiation, SH-RML efficiently optimizes the RML cost function, which is designed to align the model predictions with observed data.

$$J(z_j) = (z_j - z_j^{\text{prior}})^T C_{ZZ}^{-1} (z_j - z_j^{\text{prior}}) + (G(z_j) - d_j)^T C_{DD}^{-1} (G(z_j) - d_j), \tag{6}$$

- **High-Fidelity Finalization**: Post optimization, the surrogate-based results are refined using the high-fidelity DARTS simulations to ensure the physical accuracy of the assimilated parameters.

The integration of ML surrogates into the RML method not only speeds up the optimization process but also circumvents the need for adjoint models typically required for gradient computations in traditional variational DA approaches.

Results

This section presents the comparative results of employing ESMDA, SH-ESMDA, and SH-RML for history matching in the context of geological CO_2 storage. We discuss the performance of each method in terms of pressure matching, uncertainty quantification, and computational efficiency, and provide insights into the implications of these results for improving CO_2 storage operations.

To perform history matching, we created a reference permeability model, generated outside our prior distribution, to create synthetic observed data. Figure 9 showcases the prior ensemble pressure response at the four monitoring points considered for data assimilation, using 100 prior models. The left panel provides a spatial representation of the monitoring points relative to the central injection well. The four plots on the right display the pressure evolution over time at each monitoring point. Each gray line represents the pressure response of an individual prior model, highlighting the variability in the prior ensemble.

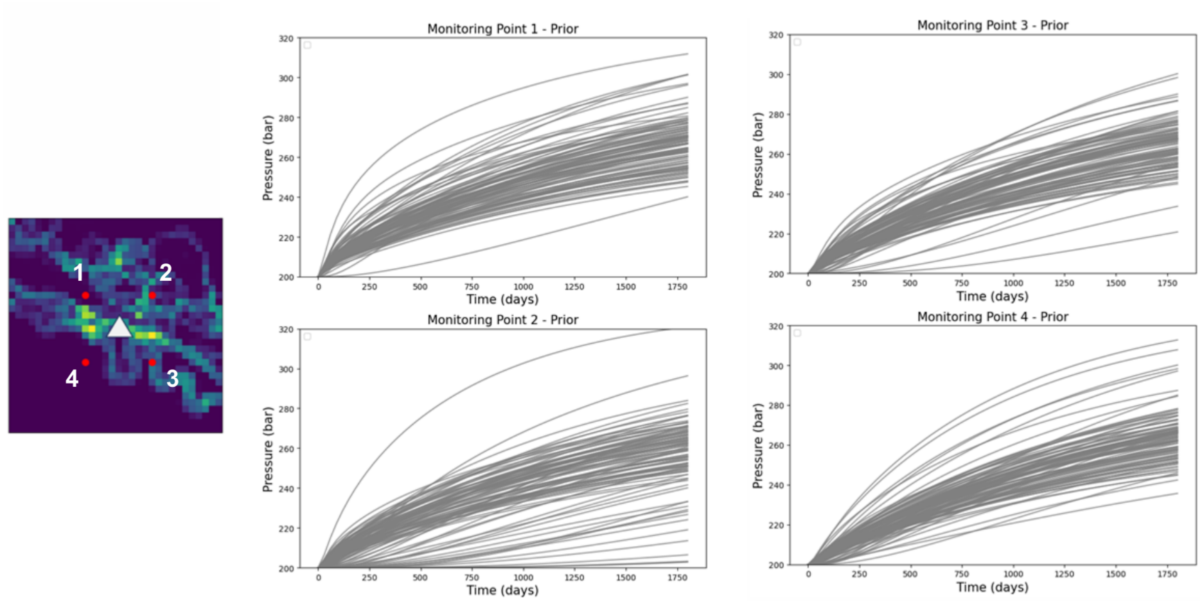

__Figure 9__ Prior ensemble pressure response at four monitoring points using 100 prior models. The left panel shows the location of the monitoring points around the central injection well. The right panels display the pressure evolution over time at each monitoring point.

First, we evaluate ESMDA, which reduced the uncertainty in pressure estimations at the monitoring points Figure 10 displays this improvement, comparing pressures from the prior, the reference model, and the posterior. We further analyze the sensitivity of the method to the number of steps in ESMDA at the monitoring pressure points for both the prior and posterior models by varying the number of ESMDA steps: 4, 8, 16, and 32. Figure 11 reveals that increasing the number of iterations does not substantially improve the quality of history matching.

In terms of uncertainty quantification, ESMDA effectively narrowed the range of uncertainty in pressure estimations after the history matching process. The true pressures observed at the monitoring points are as follows: 255.1 bar at Monitoring Point 1, 252.0 bar at Monitoring Point 2, 255.0 bar at Monitoring Point 3, and 251.4 bar at Monitoring Point 4. By analyzing the pressure distributions at the final injection step, we observed a significant variance reduction between the prior and the posterior, which indicates a decrease in the uncertainty of pressure buildup within the reservoir. The quantitative assessment of this reduction is depicted in the P10-P90 pressure range, which serves as an indicator of uncertainty. The range narrowed significantly post-history matching, showing a decrease in the spread of estimated pressures, enhancing the predictive accuracy of the model. Specifically, Monitoring Point 1 saw a decrease from a prior range of 213.9–268.8 bar to a posterior range of 212.6–261.1 bar, Monitoring Point 2 from 202.7–261.2 bar to 211.0–259.9 bar, Monitoring Point 3 from 209.9–265.1 bar to 211.5–260.2 bar, and

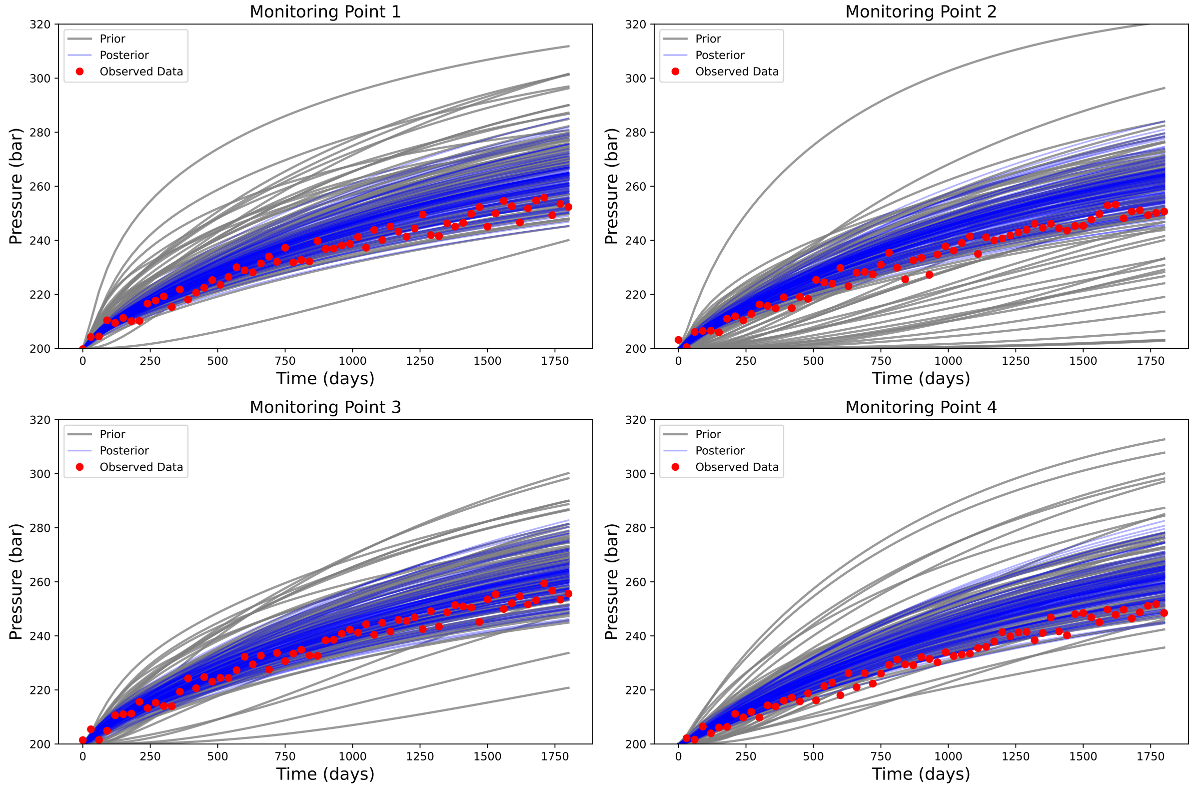

__Figure 10__ Comparison between the prior, reference model, and posterior pressures at each monitoring point for the ESMDA history matching. Red dots represent a realization of perturbed observed data.

Monitoring Point 4 from 208.7–264.0 bar to 208.8–259.0 bar. These reductions show that ESMDA is reducing the uncertainty associated with pressure estimations in reservoir modeling.

Although ESMDA reduces errors related to measured pressure in comparison to the prior, it significantly overestimates reservoir permeability in comparison to prior permeability distributions, as illustrated in Figure 12. While undesirable, the discrepancy can be explained by the fact that history matching is an ill-posed problem, allowing for multiple solutions that can satisfactorily fit the data.

Following the analysis of ESMDA, we now focus on the performance of the hybrid methods, SH-ESMDA and SH-RML. These methods integrate machine learning surrogates to enhance the efficiency and accuracy of the history matching. Figure 13 presents the history matching results for the first monitoring point for both SH-ESMDA and SH-RML methods, utilizing both T-UNet and FNO as surrogates. As observed, the SH-ESMDA methods yield results similar to ESMDA, effectively reducing the uncertainty in pressure predictions. SH-RML methods exhibit superior results, achieving a closer match to the observed data, which suggests an improvement in capturing the complex dynamics of the reservoir. The detailed results for other monitoring points are provided in the Appendix.

The improvements in history matching are quantitatively supported by the uncertainty reduction depicted in Table 1, which summarizes the P10-P90 pressure range reductions across all methods and monitoring points.

Given the inherent assumptions of ESMDA, namely, its reliance on Gaussian distributions and its better suitability for linear problems—none of which are present in our case—it is crucial to recognize its limitations in addressing the ill-posed problems we encounter. Our subsequent results delve into hybrid methods, as detailed in Section **??**. These techniques serve dual purposes: one aims to accelerate the computational process, while the other focuses on enhancing the accuracy of history matching.

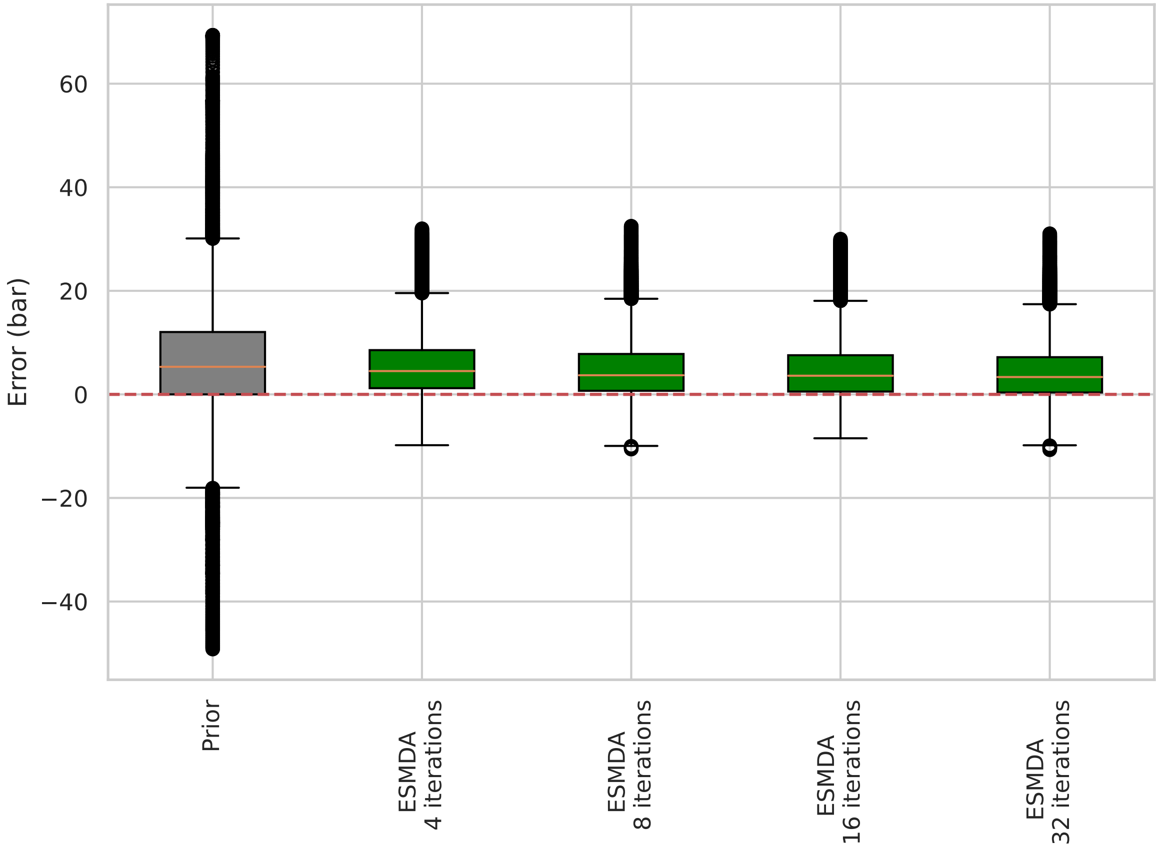

Figure 11 *Comparison of monitoring pressure absolute error across different ESMDA iterations and the prior. Red dots represent a realization of perturbed observed data.*

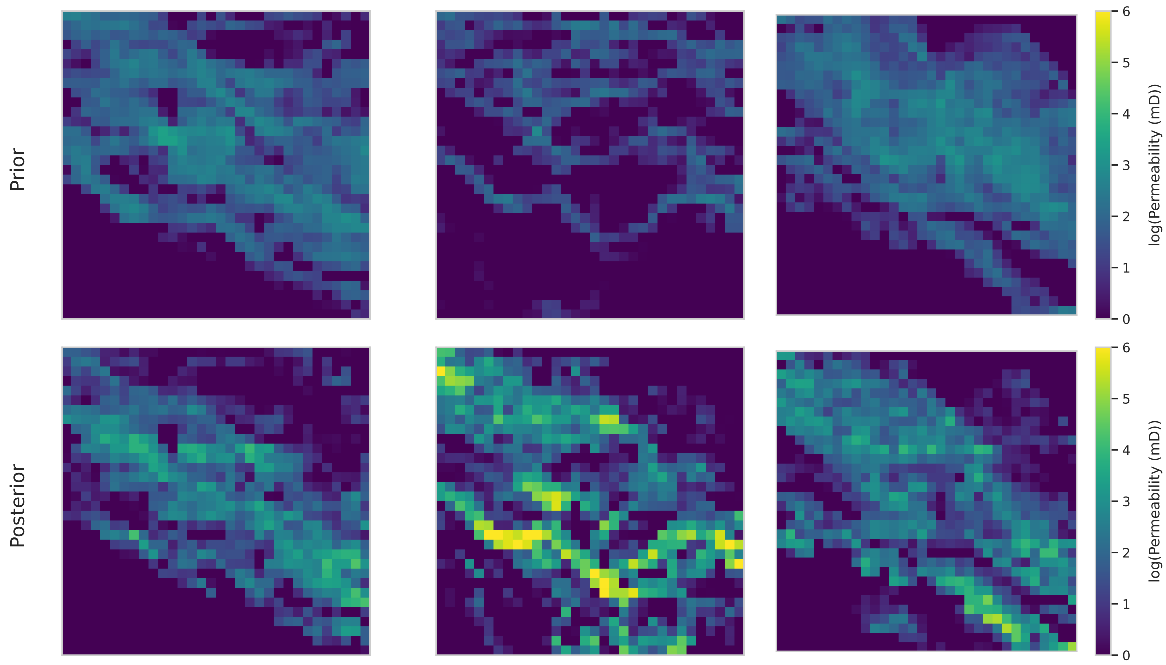

Figure 12 *Comparison between prior and posterior permeabilities across three different samples for the ESMDA.*

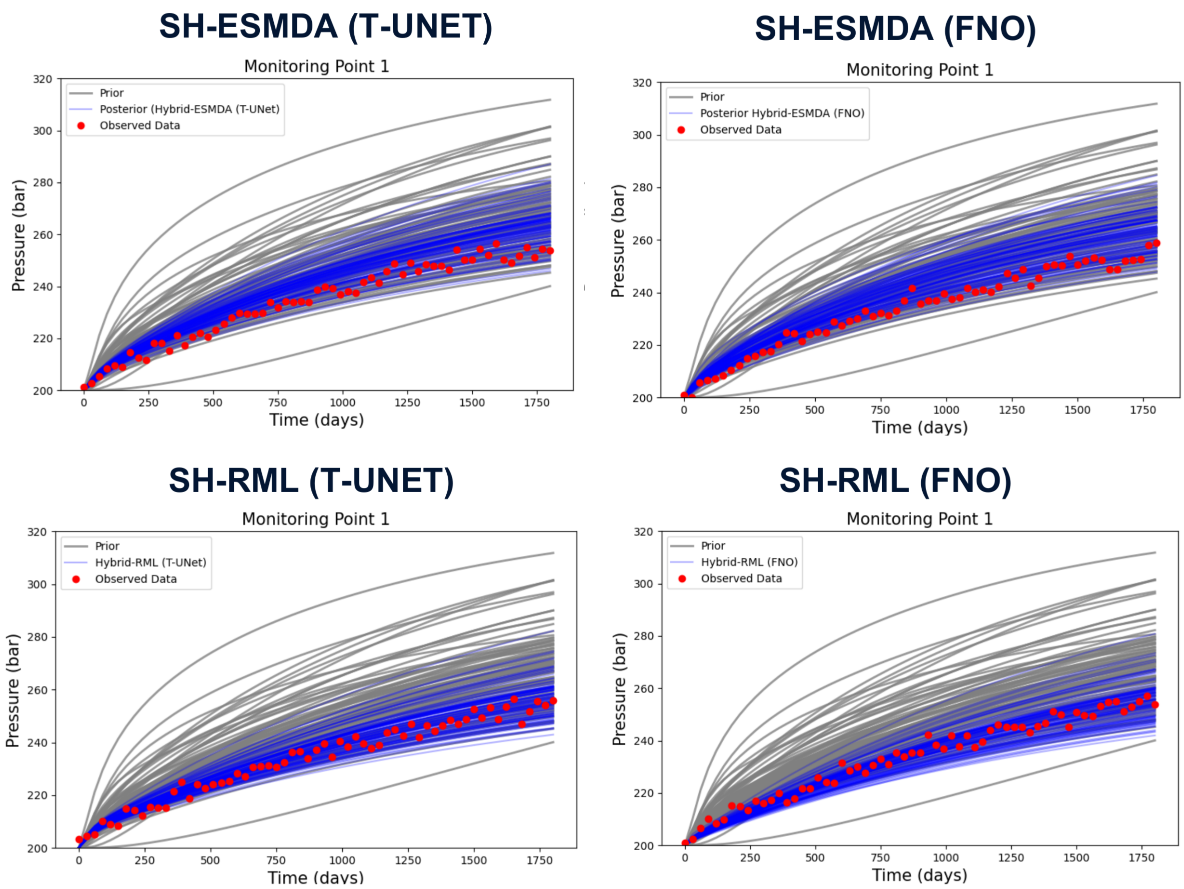

Figure 13 *History matching results at Monitoring Point 1 for SH-ESMDA and SH-RML methods using both T-UNet and FNO surrogates.*

Table 1 *Uncertainty reduction in P10-P90 pressure range at monitoring points for the ESMDA, SH-ESMDA and SH-RML history matching.*

Location	Prior (bar)		Posterior (bar)	
	P10-P90	**Difference**	**P10-P90**	**Difference**
		ESMDA		
1	213.9 - 268.8	54.9	212.6 - 261.1	48.5
2	202.7 - 261.2	58.4	211.0 - 259.9	48.9
3	209.9 - 265.1	55.2	211.5 - 260.2	48.7
4	208.7 - 264.0	55.3	208.8 - 259.0	50.2
		SH-ESMDA		
1	213.9 - 268.8	54.9	212.96 - 262.1	49.14
2	202.7 - 261.2	58.4	210.93 - 260.8	49.87
3	209.9 - 265.1	55.2	211.65 - 261.0	49.39
4	208.7 - 264.0	55.3	209.10 - 260.1	50.97
		SH-RML		
1	213.9 - 268.8	54.9	209.0 - 253.9	44.9
2	202.7 - 261.2	58.4	208.7 - 253.7	45.0
3	209.9 - 265.1	55.2	208.2 - 253.5	45.3
4	208.7 - 264.0	55.3	208.2 - 253.5	45.3

A significant advantage of SH-ESMDA is the substantial reduction in computational time. Figure 14 illustrates the runtime comparison across different methods, clearly demonstrating the efficiency gains achieved with SH-ESMDA. Both the FNO and T-UNet surrogates significantly accelerate the computation compared to the standard ESMDA method. This acceleration is particularly pronounced as the number of steps increases, with the hybrid methods maintaining relatively stable computational times even as the complexity grows. For instance, at 16 steps, standard ESMDA requires 303 minutes, while SH-ESMDA with FNO and T-UNet surrogates completes the task in just 58 and 55 minutes, respectively. This dramatic reduction in processing time, approximately 80% for the most complex case, makes SH-ESMDA particularly suitable for larger-scale or more frequent analyses in practical GCS applications.

However, similar to ESMDA, SH-ESMDA tends to overestimate the permeability field, a limitation that stems from the method's reliance on the ESMDA framework. In contrast to SH-ESMDA, SH-RML not only provides better history matching but also offers improved estimations of permeability fields. Figure 15 illustrates the posterior permeability fields obtained with the SH-RML method using FNO surrogates, showing a more realistic estimation that closely aligns with the prior distributions.

Building upon these results, our research adds valuable insights to the existing knowledge on integrating machine learning with data assimilation in the context of geological carbon storage. This aligns with the data learning methodologies framework proposed by Buizza et al. (2022) and expands on the collective research efforts, such as those by Tang et al. (2022) and Wen et al. (2021b), which also utilize machine learning models to enhance data assimilation processes. Our study sets itself apart by maintaining physics consistency in the posterior, addressing a significant limitation found in previous works where reliance on surrogate models often overlooked this crucial aspect (Tang et al., 2022; Wen et al., 2021b). Moreover, we explore the innovative application of combining transformers with UNets for CO_2 storage challenges, as suggested by Li et al. (2023). This adaptation highlights the flexibility and capability of advanced neural network architectures to manage the complex spatial and temporal data patterns typically found in subsurface environments. Furthermore, by employing FNOs, we successfully address the challenge of data demands for model training—a persistent issue in related studies Wen et al. (2021a); Tang et al. (2022); Sun and Durlofsky (2019). Our methods not only minimize the data required but also significantly enhance the computational efficiency of the data assimilation framework, providing a robust solution to one of the principal obstacles in applying deep learning techniques to geosciences.

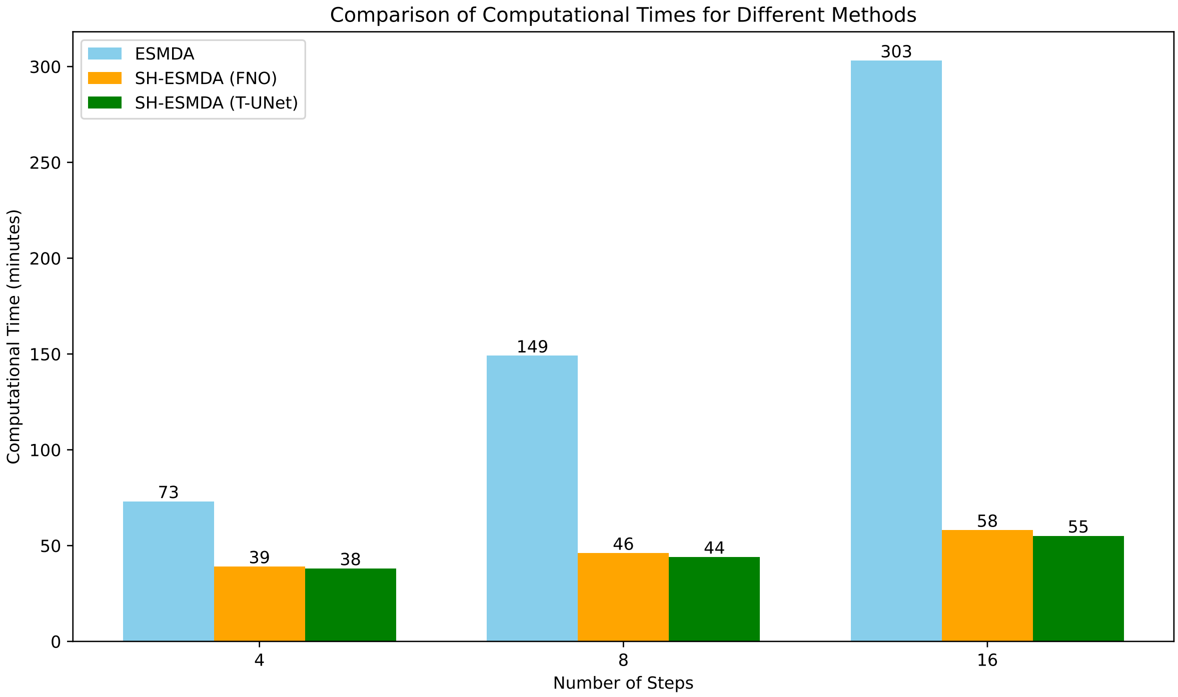

Figure 14 *Comparison of computational times for ESMDA and SH-ESMDA methods using FNO and T-UNet surrogates. The bar chart shows the runtime in minutes for different numbers of assimilation steps, demonstrating the significant time savings achieved by the hybrid methods.*

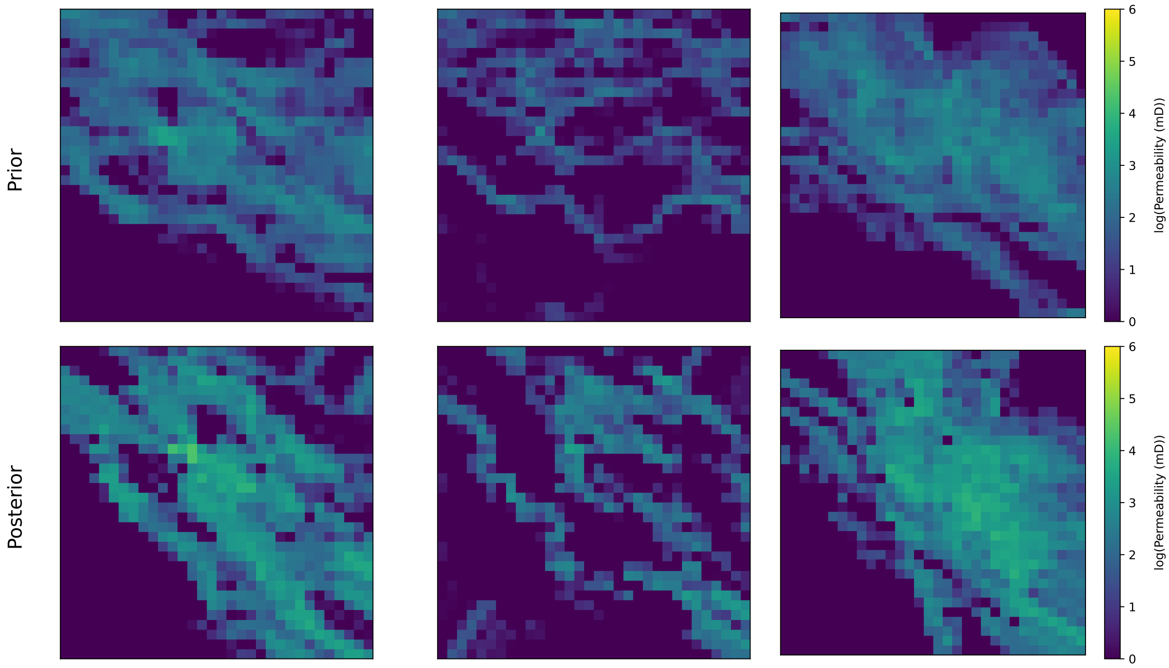

Figure 15 *Posterior permeabilities for Hybrid-RML-Surrogate with FNO surrogates.*

Discussion

This study explores DA and ML integration, advancing history matching for CO_2 storage projects. Our frameworks, namely SH-ESMDA and SH-RML, optimize computational efficiency and accuracy in DA applications by incorporating ML surrogates. SH-ESMDA accelerates the computations of Ensemble Smoother with Multiple Data Assimilation (ESMDA), maintaining consistent physical responses, whereas SH-RML excels in providing superior history matching through improved gradient approximations enabled by ML automatic differentiation. Although initially limited by computational resources affecting grid resolution, subsequent enhancements have allowed for exploration at higher resolutions. Both frameworks ensure the physical reliability of outputs via the DARTS simulator, though their effectiveness hinges on the precision of ML surrogates, which poses challenges for uncertainty quantification. Addressing these limitations may involve developing more robust nonlinear DA methods and refining ML surrogate training for enhanced reliability in gradient computation. The study demonstrates the frameworks' suitability across different applications, emphasizing their potential in geothermal energy and nuclear waste disposal.

Conclusion

We introduced innovative frameworks that integrate ML with DA to improve uncertainty quantification in Geological Carbon Storage (GCS) projects. Comparative analyses favored the Fourier Neural Operators (FNOs) over Transformer-UNet (T-UNet) in scenarios with limited training data. Employing these surrogates, hybrid methods—SH-ESMDA and SH-RML—not only reduce computational times by over 50% but also enhance accuracy in history matching. SH-RML, in particular, demonstrated an improvement in uncertainty quantification, facilitated by efficient gradient computations from FNO. This integration of ML efficiency with the physical reliability of reservoir simulators paves the way for scaling our methods to more extensive and complex reservoir systems, potentially optimizing real-world GCS operations. Future directions include expanding the scalability of our methodologies to include additional neural network architectures for broader applications beyond CO_2 sequestration, such as geothermal energy and nuclear waste management. This study not only marks significant progress in integrating AI with DA for GCS but also sets the stage for further research in enhancing operations across various subsurface modeling applications.

Acknowledgment

The authors thank Petróleo Brasileiro S.A. (Petrobras) for sponsoring the doctoral research of Gabriel Serrão Seabra and Vinicius Luiz Santos Silva.

We also thank Guillaume Rongier for providing valuable insights on geological modeling, Alexandre Emerick and Rafael Oliveira for sharing expertise on data assimilation techniques, and Ahmed ElSheikh for fruitful discussions about the machine learning models.

References

Agogo, O., Gosselin, O., Aanonsen, S.I. and Navdal, J. [2022] Ensemble Data Space Inversion for Fast CO_2 Injection Forecast Evaluation. *Energy Procedia*, **159**, 111–117.

AlSalmi, H. and Elsheikh, A.H. [2023] Automated seismic semantic segmentation using Attention U-Net. *GEOPHYSICS*, 1–75.

Brajard, J., Carrassi, A., Bocquet, M. and Bertino, L. [2021] Combining data assimilation and machine learning to infer unresolved scale parametrization. *Philosophical Transactions of the Royal Society A: Mathematical, Physical and Engineering Sciences*, **379**(2194), 20200086.

de Brito, D.U. and Durlofsky, L.J. [2020] Field development optimization using a sequence of surrogate treatments. *Computational Geosciences*, **25**(1), 35–65.

Buizza, C., Casas, C.Q., Nadler, P., Mack, J., Marrone, S., Titus, Z., Cornec, C.L., Heylen, E., Dur, T., Ruiz, L.B., Heaney, C., Lopez, J.A.D., Kumar, K.S. and Arcucci, R. [2022] Data Learning: Integrating Data Assimilation and Machine Learning. *Journal of Computational Science*, **58**, 101525.

Burchette, T.P. [2012] Carbonate rocks and petroleum reservoirs: a geological perspective from the industry. *Geological Society, London, Special Publications*, **370**(1), 17–37.

Chen, Y. and Voskov, D. [2020] Optimization of CO2 injection using multi-scale reconstruction of composition transport. *Computational Geosciences*, **24**(2), 819–835.

Cheng, S., Quilodran-Casas, C., Ouala, S., Farchi, A., Liu, C., Tandeo, P., Fablet, R., Lucor, D., Iooss, B., Brajard, J., Xiao, D., Janjic, T., Ding, W., Guo, Y., Carrassi, A., Bocquet, M. and Arcucci, R. [2023] Machine learning with data assimilation and uncertainty quantification for dynamical systems: a review.

CMG [2023] Reservoir Simulation Software. `https://www.cmgl.ca/`. [Accessed 30 August 2023].

DARTS [2024] open-DARTS repository.

Dong, Z., Cheng, J., Liu, T., Si, G. and Ma, B. [2021] A Novel Surface Parametric Method and Its Application to Aerodynamic Design Optimization of Axial Compressors. *Processes*, **9**(7), 1230.

DuMux [2023] DuMux Simulator. `https://dumux.org`. [Accessed 30 August 2023].

Emerick, A.A. and Reynolds, A.C. [2013a] Ensemble Smoother with Multiple Data Assimilation. *Computers & Geosciences*, **55**, 3–15.

Emerick, A.A. and Reynolds, A.C. [2013b] Investigation of the sampling performance of ensemble-based methods with a simple reservoir model. *Computational Geosciences*, **17**(2), 325–350.

Evensen, G., Vossepoel, F.C. and van Leeuwen, P.J. [2022] *Data Assimilation Fundamentals: A Unified Formulation of the State and Parameter Estimation Problem*. Springer Textbooks in Earth Sciences, Geography and Environment. Springer International Publishing, Cham.

Fenghour, A., Wakeham, W.A. and Vesovic, V. [1998] The viscosity of carbon dioxide. *Journal of physical and chemical reference data*, **27**(1), 31–44.

Geneva, N. and Zabaras, N. [2022] Transformers for modeling physical systems. *Neural Networks*, **146**, 272–289.

GEOSX [2023] GEOSX Simulator. `https://geosx.org`. [Accessed 8 March 2023].

Hesthaven, J.S., Rozza, G., Stamm, B. et al. [2016] *Certified reduced basis methods for parametrized partial differential equations*, 590. Springer.

IEA [2022] Carbon Capture, Utilisation and Storage - Fuels & Technologies. Tech. rep., International Energy Agency.

Khait, M. and Voskov, D.V. [2017] Operator-based linearization for general purpose reservoir simulation. *Journal of Petroleum Science and Engineering*, **157**, 990–998.

Kingma, D.P. and Ba, J. [2014] Adam: A method for stochastic optimization. *arXiv preprint arXiv:1412.6980*.

Korondi, P.Z., Marchi, M., Parussini, L. and Poloni, C. [2020] Multi-fidelity design optimisation strategy under uncertainty with limited computational budget. *Optimization and Engineering*, **22**(2), 1039–1064.

Li, G., Jin, D., Yu, Q. and Qi, M. [2023] IB-TransUNet: Combining Information Bottleneck and Transformer for Medical Image Segmentation. *Journal of King Saud University - Computer and Information Sciences*, **35**(3), 249–258.

Li, Q. and Liu, G. [2016] Risk assessment of the geological storage of CO2: A review. *Geologic carbon sequestration: Understanding reservoir behavior*, 249–284.

Li, Z., Kovachki, N., Azizzadenesheli, K., Liu, B., Bhattacharya, K., Stuart, A. and Anandkumar, A. [2020] Fourier Neural Operator for Parametric Partial Differential Equations.

Lyu, X. and Voskov, D. [2023] Advanced modeling of enhanced CO2 dissolution trapping in saline aquifers. *International Journal of Greenhouse Gas Control*, **127**, 103907.

Machado, M.V.B., Delshad, M. and Sepehrnoori, K. [2023] Potential Benefits of Horizontal Wells for CO2 Injection to Enhance Storage Security and Reduce Leakage Risks. *Applied Sciences*, **13**(23), 12830.

March, R., Doster, F. and Geiger, S. [2018] Assessment of CO_2 Storage Potential in Naturally Fractured Reservoirs With Dual-Porosity Models. *Water Resources Research*, **54**(3), 1650–1668.

Mücke, N.T., Bohté, S.M. and Oosterlee, C.W. [2021] Reduced order modeling for parameterized time-dependent PDEs using spatially and memory aware deep learning. *Journal of Computational Science*, **53**, 101408.

Nunes, J.P.P., Seabra, G.S., do Amaral, R.F. and de Sousa Junior, L.C. [2022] CCS in the Brazilian Pre-Salt: Current Status and Geomechanical Considerations. 22. Instituto Brasileiro de Petroleo e Gas,

441–442.
Ohlberger, M. and Rave, S. [2015] Reduced basis methods: Success, limitations and future challenges. *arXiv preprint arXiv:1511.02021*.
Oliver, D.S., He, N. and Reynolds, A.C. [1996] Conditioning Permeability Fields to Pressure Data. In: *ECMOR V - 5th European Conference on the Mathematics of Oil Recovery*. European Association of Geoscientists & Engineers.
Pintea, S.L., Sharma, S., Vossepoel, F.C., van Gemert, J.C., Loog, M. and Verschuur, D.J. [2021] Seismic inversion with deep learning. *Computational Geosciences*, **26**(2), 351–364.
Pour, K.M., Voskov, D. and Bruhn, D. [2023] Nonlinear solver based on trust region approximation for CO2 utilization and storage in subsurface reservoir. *Geoenergy Science and Engineering*, **225**, 211698.
Pyrcz, M., Boisvert, J. and Deutsch, C. [2009] ALLUVSIM: A program for event-based stochastic modeling of fluvial depositional systems. *Computers & Geosciences*, **35**(8), 1671–1685.
Quarteroni, A., Manzoni, A. and Negri, F. [2015] *Reduced basis methods for partial differential equations: an introduction*, 92. Springer.
Ringrose, P.S. and Meckel, T.A. [2019] Maturing global CO2 storage resources on offshore continental margins to achieve 2DS emissions reductions. *Scientific Reports*, **9**(1).
Ronneberger, O., Fischer, P. and Brox, T. [2015] U-net: Convolutional networks for biomedical image segmentation. In: *Medical Image Computing and Computer-Assisted Intervention–MICCAI 2015: 18th International Conference, Munich, Germany, October 5-9, 2015, Proceedings, Part III*, 18. Springer International Publishing, 234–241.
Rutqvist, J. [2012] The geomechanics of CO2 storage in deep sedimentary formations. *Geotechnical and Geological Engineering*, **30**, 525–551.
Schlumberger [2023] ECLIPSE Reservoir Simulator. `https://www.slb.com/reservoir-characterization-and-simulation/software/eclipse`. [Accessed 30 August 2023].
Seabra, G., Mücke, N., Silva, V., Voskov, D. and Vossepoel, F. [2024] AI enhanced data assimilation and uncertainty quantification applied to Geological Carbon Storage. *arXiv preprint arXiv:2402.06110*.
Silva, V.L.S., Heaney, C.E. and Pain, C.C. [2023] Generative network-based reduced-order model for prediction, data assimilation and uncertainty quantification. In: *LatinX in AI Workshop at International Conference on Machine Learning*.
Sun, A.Y. and Durlofsky, L.J. [2019] An Integrated Framework for Optimal Monitoring and History Matching in CO_2 Storage Projects. *Energy Procedia*, **159**, 103–110.
Taccari, M.L., Nuttall, J., Chen, X., Wang, H., Minnema, B. and Jimack, P.K. [2022] Attention U-Net as a surrogate model for groundwater prediction. *Advances in Water Resources*, **163**, 104169.
Tadjer, A. and Bratvold, R.B. [2021] Managing uncertainty in geological CO2 storage using Bayesian evidential learning. *Energies*, **14**(6), 1557.
Tang, G., Wen, J., Ma, X., Feng, Y., Wu, Y. and Durlofsky, L.J. [2022] Deep-learning-based coupled flow-geomechanics surrogate model for CO_2 sequestration. *International Journal of Greenhouse Gas Control*, **118**, 103692.
Tang, H. and Durlofsky, L.J. [2022] Use of low-fidelity models with machine-learning error correction for well placement optimization. *Computational Geosciences*, **26**(5), 1189–1206.
Tarantola, A. [2005] *Inverse Problem Theory and Methods for Model Parameter Estimation*. Other Titles in Applied Mathematics. Society for Industrial and Applied Mathematics.
Tarrahi, M., Jafarpour, B. and Ghassemi, A. [2015] Integration of microseismic monitoring data into coupled flow and geomechanical models with ensemble Kalman filter. *Water Resources Research*, **51**(7), 5245–5260.
Tian, X., Volkov, O. and Voskov, D. [2024a] An advanced inverse modeling framework for efficient and flexible adjoint-based history matching of geothermal fields. *Geothermics*, **116**, 102849.
Tian, X., Wapperom, M., Gunning, J., Jackson, S., Wilkins, A., Green, C., Ennis-King, J. and Voskov, D. [2024b] A history matching study for the fluidflower benchmark project. *Transport in Porous Media*, 1–27.
Wapperom, M., Tian, X., Novikov, A. and Voskov, D. [2023] FluidFlower benchmark: lessons learned from the perspective of subsurface simulation. *Transport in Porous Media*, 1–20.
Wen, G., Li, Z., Azizzadenesheli, K., Anandkumar, A. and Benson, S.M. [2022] U-FNO—An enhanced Fourier neural operator-based deep-learning model for multiphase flow. *Advances in Water Resources*,

163, 104180.
Wen, G., Tang, M. and Benson, S.M. [2021a] Towards a predictor for CO2 plume migration using deep neural networks. *International Journal of Greenhouse Gas Control*, **105**, 103223.
Wen, J., Wu, Y., Durlofsky, L.J., Ma, X., Tang, G. and Feng, Y. [2021b] A deep learning-accelerated data assimilation and forecasting workflow for commercial-scale geologic carbon storage. *International Journal of Greenhouse Gas Control*, **109**, 103488.
White, J.A. and Foxall, W. [2016] Assessing induced seismicity risk at CO2 storage projects: Recent progress and remaining challenges. *International Journal of Greenhouse Gas Control*, **49**, 413–424.
Witte, P.A., Konuk, T., Skjetne, E. and Chandra, R. [2023] Fast CO_2 saturation simulations on large-scale geomodels with artificial intelligence-based Wavelet Neural Operators. *International Journal of Greenhouse Gas Control*, **126**, 103880.
Zhang, C., Song, X. and Azevedo, L. [2021] U-net generative adversarial network for subsurface facies modeling. *Computational Geosciences*, **25**(1), 553–573.
Zoback, M.D. and Gorelick, S.M. [2012] Earthquake triggering and large-scale geologic storage of carbon dioxide. *Proceedings of the National Academy of Sciences*, **109**(26), 10164–10168.

Appendix

This appendix presents a detailed discussion and comparative figures illustrating monitoring pressure results from various history matching methods employed in this study. The integration of machine learning surrogates, specifically Fourier Neural Operators (FNO), into the ESMDA framework aims to enhance computational efficiency while maintaining the accuracy of standard ESMDA. This hybrid method leverages the strengths of both traditional data assimilation techniques and advanced machine learning models. As shown in Figure 16, the FNO surrogate captures the dynamics of the reservoir effectively, aligning closely with the results from the standard ESMDA method, thus confirming the surrogate's ability to replicate complex physical processes accurately.

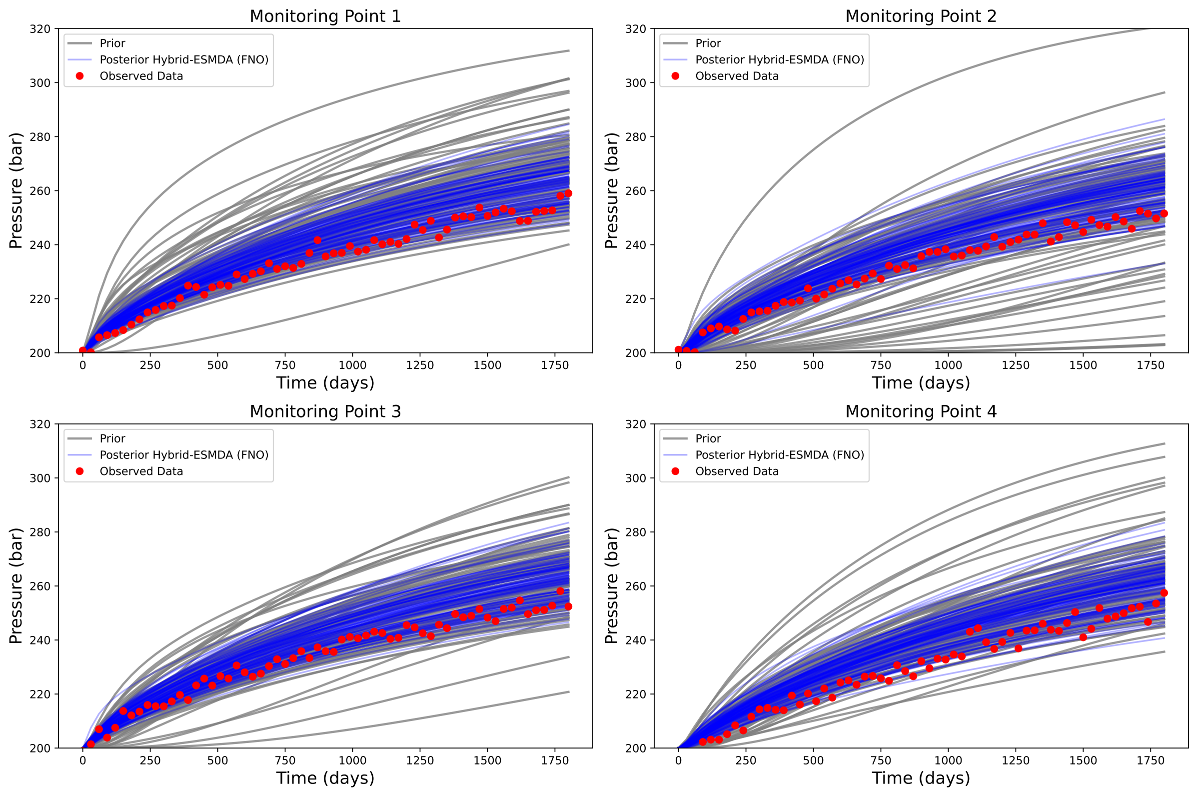

Figure 16 *Pressure comparison at monitoring points for Hybrid ESMDA using FNO surrogate. Red dots represent a realization of perturbed observed data.*

Continuing the exploration of machine learning surrogates, the T-UNet model is evaluated for its efficacy in the ESMDA setup. Similar to FNO, T-UNet is expected to provide a balance between computational speed and history matching accuracy. Figure 17 illustrates that T-UNet, while slightly less accurate than FNO in some cases, still provides a substantial improvement over the priors.

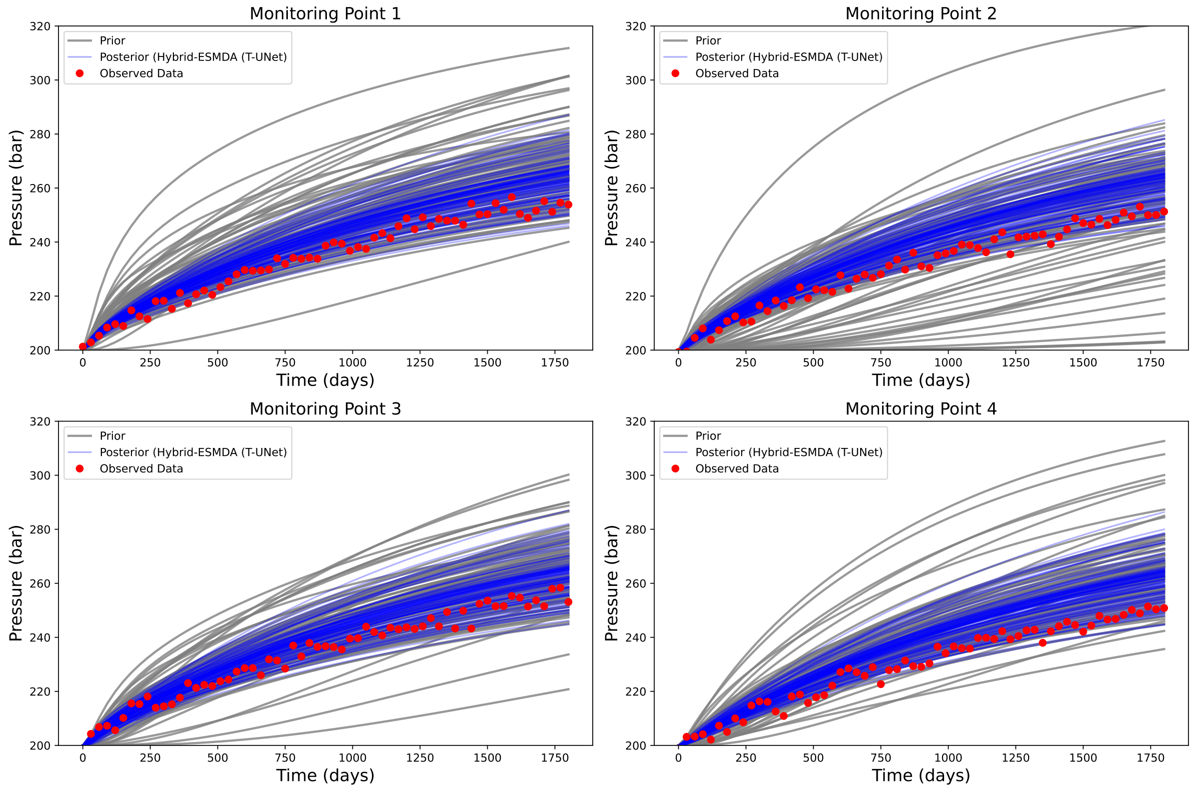

Figure 17 *Pressure comparison at monitoring points for Hybrid ESMDA using T-UNet surrogate. Red dots represent a realization of perturbed observed data.*

The SH-RML approach represents a further step in the use of machine learning within the data assimilation framework. It employs machine learning surrogates, specifically for gradient evaluation, enhancing the optimization process in reservoir simulations. Figure 18 displays the outcomes from employing the FNO surrogate within the SH-RML framework. The results underscore the efficacy of SH-RML in closely aligning the simulated pressures with the observed data, thereby validating the surrogate's role in maintaining high fidelity in model predictions. This is particularly evident in the way SH-RML handles the complex dynamics of the reservoir, which are often challenging to capture with traditional methods. Similarly, Figure 19 shows the application of the T-UNet model within the same SH-RML framework. The T-UNet surrogate, while demonstrating a slight variance from the FNO results, still significantly enhances the model's performance compared to traditional simulations.

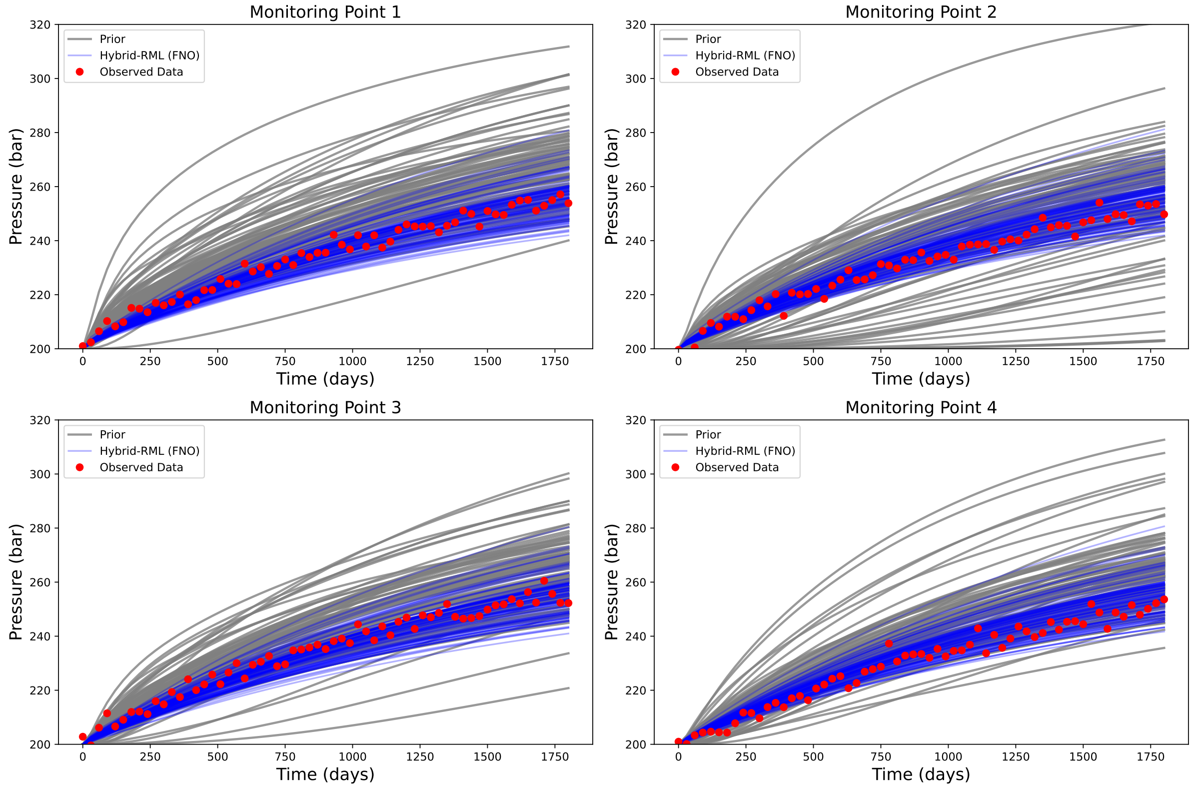

Figure 18 *Pressure comparison at each monitoring point for SH-RML using FNO surrogates. Red dots represent a realization of perturbed observed data, highlighting the accuracy of SH-RML in matching observed data closely.*

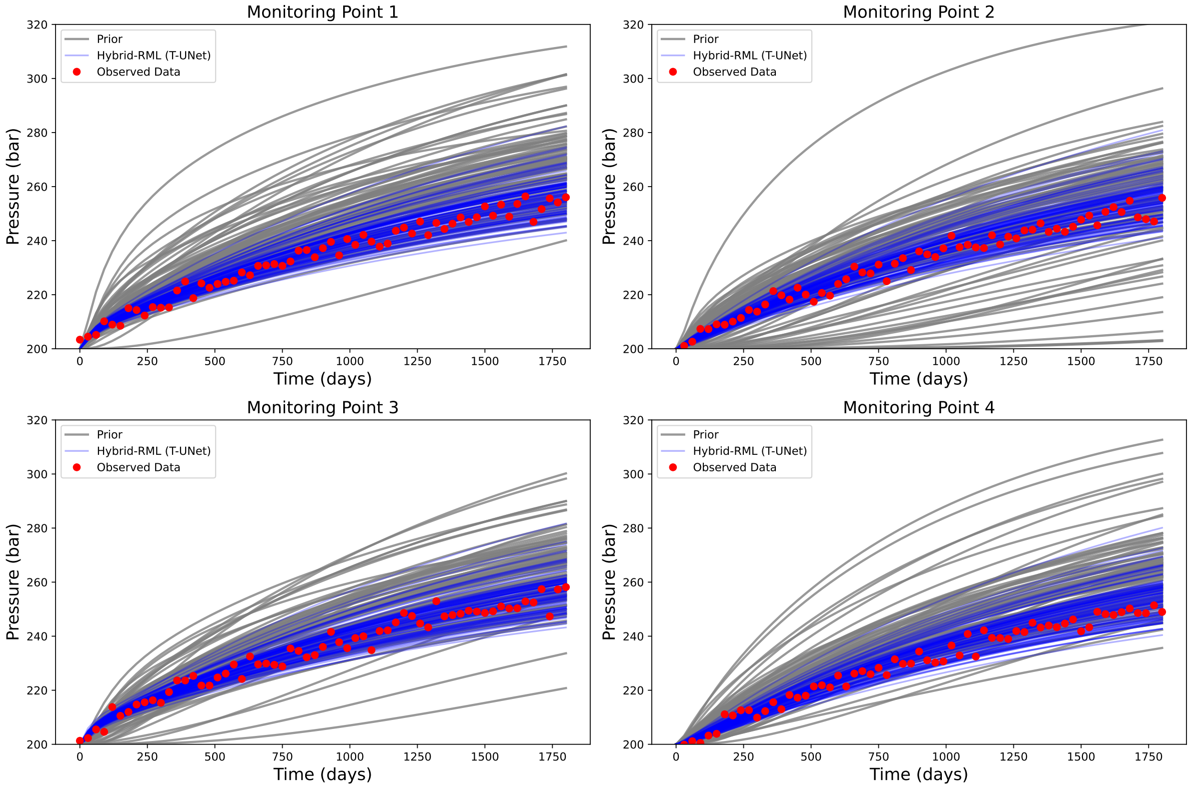

Figure 19 *Comparison of monitoring pressure results using T-UNet surrogates in SH-RML. This figure illustrates the surrogate's capability to adhere to the accuracy requirements while enabling faster computational times.*